

Modeling of an MHD Free Surface Problem Arising in CZ Crystal Growth

R. Griesse, Faculty of Mathematics, Chemnitz University of Technology, D–09107
Chemnitz, Germany

A. J. Meir, Department of Mathematics and Statistics, Auburn University, Auburn,
AL 36849–5310, USA

(August 26, 2008)

A free surface problem arising in the Czochralski (CZ) crystal growth process is considered. A mathematical model accounting for the interaction of the molten material with applied and induced magnetic fields, temperature-induced convection, rotating boundaries and a free surface is given. The model described avoids some common simplifying assumptions and allows for more general geometries, and non axisymmetric (fully three-dimensional) and time-dependent flow fields. It accounts for the induced magnetic field and avoids nonrealistic idealized boundary conditions on the magnetic field. The use and limitations of the model in optimization of crystal growth are also discussed.

Keywords: magnetohydrodynamics; mathematical modeling; free surface; crystal growth; Czochralski process

AMS Subject Classification: 76W05, 76D27, 76D55

1 Introduction

In this paper we consider some aspects concerning the mathematical modeling of free surface problems arising in technical processes which involve the interaction of electrically conducting fluids and magnetic fields, described by the equations of magnetohydrodynamics (MHD). To focus the discussion, we restrict ourselves to the Czochralski (CZ) process in crystal growth. However, our model can be readily extended to, e.g., continuous casting problems which are described in [1, 3, 29, 30], and the references therein, and to aluminum reduction cells, see, e.g., [2, 6, 8].

The CZ crystal growth process is used, for instance, to grow silicon crystals for the semiconductor industry. The silicon is melted inside a crucible before a seed is lowered into the melt to initiate the crystallization process. The seed is slowly pulled upwards, and the pulling speed determines the diameter of the

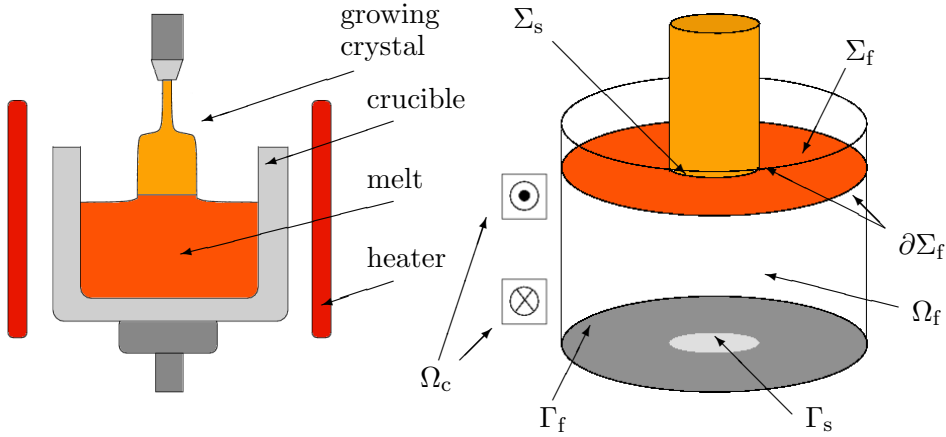


Figure 1. Schematic of the CZ process and geometry of the free surface problem.

ingot. A schematic of the CZ process is shown in Figure 1. For a review paper describing this process, we refer to [27].

Due to temperature gradients in the hot melt, a strong buoyancy-driven flow can develop. In the presence of a free surface, surface tension and its variation with temperature also drive fluid motion, known as the Marangoni effect. In addition, both the seed and the crucible are often rotated. Rotating or steady magnetic fields may be applied to influence the fluid motion in a favorable way. Some of the concerns during the production process are non-uniform dopant distribution and impurity striations. Desired properties, in order to obtain high quality crystals, include reduction of radial and axial temperature gradients and a flow field close to an axisymmetric configuration, in order to homogenize solute concentration. In addition, it is desired to damp out flow instabilities, or to overpower turbulence which otherwise lead to deterioration of the final crystal's properties, see, e.g., [11, 13, 32–34, 37, 39, 40].

The current work differs from prior work in a number of aspects. One main feature of the model presented is the use of the electric current density rather than the magnetic field as the primary electromagnetic variable. This is known as the velocity-current formulation of the MHD equations (see [21] and [22]). Here the induced magnetic field is recovered from the current density via the Biot-Savart law making idealized or artificial electromagnetic boundary conditions unnecessary. This allows us to account for the interior and exterior magnetic fields even though the equations are posed on the (bounded) fluid and conductor regions. It also allows for coupling between the conducting fluid and external conductors (the electromagnetic principle of *action at a distance*).

In addition, we do *not* assume that the equations decouple or partially decouple, allowing for separation of fluid field, electromagnetic field, and temperature field computations. Some earlier work, in particular in the context

of crystal growth problems, is restricted to situations without such coupling and requires some unrealistic simplifying assumptions, e.g., small magnetic Reynolds number, and vessels with perfectly conducting or insulating walls. Moreover, we do not neglect the induced magnetic fields, the electromagnetic interaction of the melt with other conductors in its vicinity, or buoyancy due to temperature fluctuations.

In contrast to most prior work we do not assume that the flow is two-dimensional and allow for fully three-dimensional flows. Note that even in the very simple situation of a rotating cylinder in the presence of a transverse magnetic field, the flow is fully three-dimensional (see [23]). Hence we describe a fully coupled three-dimensional model consisting of the full system of hydrodynamic and electromagnetic equations under realistic interface conditions for the magnetic field.

This work is an extension of [10], where the stationary case was considered. In addition, we devote Section 3 to a brief discussion of the model's use and its limitations in optimization problems for crystal growth.

2 Mathematical Model

The growth of an actual crystal in practice is a tremendously complicated process, therefore we focus here only on some of the aspects, for which we give a mathematical model. In particular, we include the interaction of the conducting melt with magnetic fields, the temperature-induced convection, the free surface, and the rotation of the solidified crystal and the crucible. To emphasize these ideas we omit the detailed modeling of heat sources which are needed to maintain the melt temperature, and neglect the interaction of the magnetic fields with the crucible, the heater, and other components of an actual crystal growing device. However, the model can be generalized to account for these additional effects. We refer for instance to [14, 15, 26] for models including heat transfer by radiation and induction and their numerical realization.

Since the growth proceeds slowly and we consider only a time window $[0, t_{\text{end}}]$ of the lengthy process, we may neglect the pull velocity. The pull velocity is usually much smaller than the rotational velocity of the crucible or fluid velocity in the melt. However, we allow for a fully instationary flow, which may develop, e.g., in the presence of a transverse magnetic field, or non-constant rotational velocities of the crucible or crystal.

As shown in Figure 1, the electrically conducting fluid occupies a bounded domain $\Omega_f \subset \mathbb{R}^3$. We further assume that the fluid may be under the influence of applied magnetic fields, some of which may be the result of electric currents flowing in various conductors $\Omega_c \subset \mathbb{R}^3$. Thus the region of space we include in

this model is $\Omega = \Omega_f \cup \Omega_c \subset \mathbb{R}^3$, a bounded domain which contains the fluid domain and the various electrically conducting regions which we account for.

We further assume that the fluid partially fills a container, and the fluid region is in part bounded above by the solid crystal (the solidification front is denoted by Σ_s) and in part by a free surface Σ_f . The surface Σ_f is not prescribed and so we are dealing with a free boundary (free surface) problem. For a brief introduction to capillary surfaces see [7] and the references therein. In the configuration depicted in Figure 1, the container is cylindrical in shape. We denote by $\Gamma = \Gamma_f \cup \overline{\Gamma_s}$ the base of the container, where Γ_s is the projection of Σ_s onto the container's base and Γ_f is the projection of the free surface onto the container's base. All three, $(\Gamma, \Gamma_f, \text{ and } \Gamma_s)$ are open sets in \mathbb{R}^2 .

2.1 The Equations for a Fixed Fluid Domain

To set the stage we begin by considering the MHD equations on a fixed domain (where the fluid completely fills the container and there is no free surface). The equations, in the fluid region Ω_f , are the MHD equations, that is the Navier Stokes equations coupled to the quasi-stationary form of Maxwell's equations via Ohm's law (and the Lorentz force)

$$\rho \frac{\partial}{\partial t} \mathbf{u} - \eta \Delta \mathbf{u} + \rho (\mathbf{u} \cdot \nabla) \mathbf{u} + \nabla p - \mathbf{J} \times \mathbf{B} = \mathbf{F},$$

$$\nabla \cdot \mathbf{u} = 0.$$

Here \mathbf{u} is the fluid velocity, p the pressure, \mathbf{J} electric current density, \mathbf{B} magnetic field (actually magnetic induction), \mathbf{F} a body force (addressed later), η the fluid's dynamic viscosity, and ρ the fluid's density.

Maxwell's equations hold on all of \mathbb{R}^3

$$\nabla \times (\mu^{-1} \mathbf{B}) = \mathbf{J}, \quad \nabla \cdot \mathbf{B} = 0, \quad (1)$$

$$\nabla \times \mathbf{E} = -\frac{\partial \mathbf{B}}{\partial t}, \quad \nabla \cdot \mathbf{E} = 0, \quad (2)$$

where the charge density is neglected as is usual in the MHD approximation. Here μ is the magnetic permeability (assumed constant) and \mathbf{E} the electric field. If μ is not a constant, the Biot-Savart and vector potential formulas below need to be extended [21].

Ohm's law takes on various forms in the various sub-domains under consid-

eration

$$\mathbf{J} = \begin{cases} \sigma(\mathbf{E} + \mathbf{u} \times \mathbf{B}) & \text{in } \Omega_f, \text{ the fluid region} \\ \mathbf{J}_0 & \text{in } \Omega_c, \text{ external conductors} \\ 0 & \text{elsewhere.} \end{cases} \quad (3)$$

Here σ is the electrical conductivity of the fluid or the external conductors, respectively, and \mathbf{J}_0 is a prescribed electric current density. The current in external conductors Ω_c is usually driven by a current or voltage source. If this is included in the model, the current density in the external conductors becomes an additional unknown, and the second equation in (3) is replaced by $\mathbf{J} = \sigma\mathbf{E}$ in Ω_c . Compatible boundary conditions for the above equations are, e.g.,

$$\mathbf{u}|_{\partial\Omega_f} = \mathbf{u}_b(\mathbf{x}, t) \quad \text{with} \quad \int_{\partial\Omega_f} \mathbf{u}_b \cdot \mathbf{n} = 0 \quad (4)$$

at all times t . Throughout, \mathbf{n} will denote an outward pointing unit vector normal to the fluid domain Ω_f . Boundary condition (4) allows for rotation of the crucible. Other boundary conditions involving the stress, or a combination of stress components and velocity components may be prescribed and are needed in order to include the free surface into our model, see Section 2.2. General boundary conditions that result in well posed problems were formulated and studied in [4]. Finally, initial conditions for the fluid velocity are imposed:

$$\mathbf{u}(\mathbf{x}, 0) = \mathbf{u}_*(\mathbf{x}). \quad (5)$$

As boundary conditions for the current we have

$$\begin{aligned} \mathbf{J} \cdot \mathbf{n}|_{\partial\Omega_f} &= 0, \\ \mathbf{J} \cdot \mathbf{n}|_{\partial\Omega_c} &= 0 \end{aligned} \quad (6)$$

at all times t . In the second equation, \mathbf{n} exceptionally denotes an outward normal to Ω_c . According to (6), the fluid container and the external conductors are insulated and there is no current flow through their boundaries. In case some of the external conductors are attached to the fluid region Ω_f , these boundary conditions must be changed to ensure continuity of the current across the attached areas, see, e.g., [4, 22, 23]. As for the fluid velocity, initial conditions are given for the current density on $\Omega_f \cup \Omega_c$:

$$\mathbf{J}(\mathbf{x}, 0) = \mathbf{J}_*(\mathbf{x}). \quad (7)$$

The electric field and magnetic field must satisfy the following interface conditions:

$$\begin{aligned} [\mathbf{B} \cdot \mathbf{n}]_{\partial\Omega_f} &= 0, & [\mathbf{E}]_{\partial\Omega_f} &= 0, \\ [\mu^{-1}\mathbf{B} \times \mathbf{n}]_{\partial\Omega_f} &= -\mathbf{J}_{\partial\Omega_f}, \end{aligned}$$

where $[\cdot]_s$ denotes the jump across the surface s , and $\mathbf{J}_{\partial\Omega_f}$ is a given surface current. The surface current $\mathbf{J}_{\partial\Omega_f}$ can be assumed zero. This is evident if the fluid container is an electrical insulator. Otherwise, if the container's wall has finite thickness, we can treat it as an additional conductor, solve Ohm's law (3) there as well, and alter the boundary conditions (6) to reflect continuity of the current across the fluid/container interface.

Moreover, we have radiation conditions at infinity

$$\mathbf{B} = \mathbf{B}_\infty, \quad \mathbf{E} = \mathbf{E}_\infty.$$

In order to simplify numerical simulations for the above system, avoid having to explicitly solve Maxwell's equations on all of space, and reduce the computations so that only unknowns defined on the bounded domain Ω are involved one can employ the, so-called, velocity-current formulation, see [22]. This formulation takes into account the fact that the magnetic field \mathbf{B} is induced by the current \mathbf{J} in the fluid and in the external conductors, see (1). This induced field can be obtained by employing the Biot-Savart law,

$$\mathbf{B}(\mathbf{x}) = \mathcal{B}(\mathbf{J})(\mathbf{x}) = -\frac{\mu}{4\pi} \int_{\mathbb{R}^3} \frac{\mathbf{x} - \mathbf{y}}{|\mathbf{x} - \mathbf{y}|^3} \times \mathbf{J}(\mathbf{y}) d^3\mathbf{y}.$$

Note that since the current \mathbf{J} vanishes outside the conductors, the integral actually extends only over the bounded set $\Omega_f \cup \Omega_c$. The Biot-Savart operator ensures that

$$\begin{aligned} \nabla \times \mathbf{B} &= \mu\mathbf{J}, & \nabla \cdot \mathbf{B} &= 0 \quad \text{on } \mathbb{R}^3, \\ [\mathbf{B}]_{\partial\Omega_f} &= 0, & \mathbf{B} &= 0 \quad \text{at infinity.} \end{aligned}$$

Since $\mathcal{B}(\mathbf{J})$ is divergence-free, one may define its vector potential $\mathcal{A}(\mathbf{J})$ satisfying $\nabla \times \mathcal{A}(\mathbf{J}) = \mathcal{B}(\mathbf{J})$. To ensure uniqueness, we gauge it with $\nabla \cdot \mathcal{A}(\mathbf{J}) = 0$. Note that $\mathcal{A}(\mathbf{J})$ is explicitly given by

$$\mathcal{A}(\mathbf{J})(\mathbf{x}) = \frac{\mu}{4\pi} \int_{\mathbb{R}^3} \frac{\mathbf{J}(\mathbf{y})}{|\mathbf{x} - \mathbf{y}|} d^3\mathbf{y}.$$

From (2) it follows that $\mathbf{E} + \partial\mathcal{A}(\mathbf{J})/\partial t$ is curl-free, hence

$$\mathbf{E} + \frac{\partial\mathcal{A}(\mathbf{J})}{\partial t} = -\nabla\phi$$

for some scalar function ϕ , called the electrostatic potential. Now the equations, in the fluid region Ω_f are

$$\rho \frac{\partial}{\partial t} \mathbf{u} - \eta \Delta \mathbf{u} + \rho (\mathbf{u} \cdot \nabla) \mathbf{u} + \nabla p - \mathbf{J} \times \mathcal{B}(\mathbf{J}) = \mathbf{F}, \quad \nabla \cdot \mathbf{u} = 0, \quad (8)$$

$$\frac{\partial}{\partial t} \mathcal{A}(\mathbf{J}) + \sigma^{-1} \mathbf{J} + \nabla \phi - \mathbf{u} \times \mathcal{B}(\mathbf{J}) = 0, \quad \nabla \cdot \mathbf{J} = 0, \quad (9)$$

see [31] for their derivation and analysis.

In case an additional applied magnetic field \mathbf{B}_0 is present, such as a field generated by a permanent magnet, we replace $\mathcal{B}(\mathbf{J})$ by $\mathcal{B}(\mathbf{J}) + \mathbf{B}_0$.

In order to model convection-driven flows, we also add an equation for the temperature (energy equation) and couple it to the momentum equation using the Boussinesq approximation. That is, the density dependence on the temperature is neglected except in the buoyancy term. The right hand side of the momentum equation becomes

$$\mathbf{F} = \rho [1 - \beta(T - T_{\text{ref}})] \mathbf{g}.$$

Here T_{ref} is a reference temperature, β is the thermal expansion coefficient, and \mathbf{g} is the acceleration of gravity.

The energy equation is

$$\rho c_p \frac{\partial}{\partial t} T - \kappa \Delta T + \rho c_p (\mathbf{u} \cdot \nabla) T = Q \quad \text{in } \Omega_f, \quad (10)$$

where κ is the fluid's thermal conductivity, c_p is its specific heat at constant pressure, and Q is some heat source. The heat source can be

$$Q = \sigma^{-1} |\mathbf{J}|^2 + \frac{1}{2} \eta |\nabla \mathbf{u} + (\nabla \mathbf{u})^\top|^2 + q, \quad (11)$$

where the first term on the right is due to Joule dissipation, the second due to viscous heating, and the third can account for additional heat sources. In many situations, the first and second term in Q are negligibly small, see, e.g., [28].

The boundary condition for the temperature can of course be of Dirichlet type (prescribed temperature), Neumann type (prescribed heat flux through

the boundary), or (mixed) Robin type representing Newton's law of cooling

$$-\kappa(\nabla T) \cdot \mathbf{n} = \alpha(T - T_{\text{ext}}) \quad \text{on } \partial\Omega_f. \quad (12a)$$

The latter is a linearization of Boltzmann's law of radiation

$$-\kappa(\nabla T) \cdot \mathbf{n} = \sigma_B \varepsilon (T^4 - T_{\text{ext}}^4) \quad \text{on } \partial\Omega_f \quad (12b)$$

with Boltzmann constant σ_B and surface emissivity ε , which will be more appropriate when the relevant temperature range is large. Both terms in (12) represent local boundary conditions. However, in situations where the melt experiences significant emission of thermal energy from other parts of the growing device, a description by non-local radiation boundary conditions is more appropriate. We refer to [19] for details.

Finally, the temperature satisfies the initial condition

$$T(\mathbf{x}, 0) = T_*(\mathbf{x}). \quad (13)$$

For convenience, we write

$$T = \Theta(\mathbf{u}, \mathbf{J})$$

where Θ is the solution operator of the temperature equation (10) subject to boundary and initial conditions (12)–(13), for a given velocity and current density. Thus we write \mathbf{F} as

$$\mathbf{F} = \rho [1 - \beta(\Theta(\mathbf{u}, \mathbf{J}) - T_{\text{ref}})] \mathbf{g}. \quad (14)$$

Now the equations, in the fluid region Ω_f are

$$\rho \frac{\partial}{\partial t} \mathbf{u} - \eta \Delta \mathbf{u} + \rho(\mathbf{u} \cdot \nabla) \mathbf{u} + \nabla p - \mathbf{J} \times \mathcal{B}(\mathbf{J}) = \rho [1 - \beta(\Theta(\mathbf{u}, \mathbf{J}) - T_{\text{ref}})] \mathbf{g},$$

$$\nabla \cdot \mathbf{u} = 0,$$

$$\frac{\partial}{\partial t} \mathcal{A}(\mathbf{J}) + \sigma^{-1} \mathbf{J} + \nabla \phi - \mathbf{u} \times \mathcal{B}(\mathbf{J}) = 0,$$

$$\nabla \cdot \mathbf{J} = 0.$$

These must be complemented by appropriate boundary and initial conditions for the velocity (4)–(5) and for the current density (6)–(7). We emphasize that the various coefficients in our equations may be temperature-dependent.

In particular, this applies to the conductivity σ and the thermal conductivity κ . We also remind the reader that \mathcal{A} , \mathcal{B} and Θ are integral operators (defined above).

2.2 The Free Boundary Value Problem

We now consider the free boundary value problem where part of the fluid's top surface Σ_f is a free surface, see [7] and the references therein, as well as, [5] and [20]. To be precise, the free surface extends from the lateral container walls inward to the solidified ingot, see Figure 1. For simplicity we assume that the crystal-melt interface Σ_s is known and constant during the time window under consideration. Of course more generally one can find the position and shape of this interface by also solving the heat equation in the crystal and employing a Stefan-type condition at this interface, see, e.g., [12].

For the free surface problem, we modify the previously given boundary conditions, e.g., (12a) or (12b) and impose

$$T = T_{\text{melt}} \quad \text{on } \Sigma_s, \quad (15)$$

i.e., on the interface separating the solidified crystal from the melt, see Figure 1. Here, T_{melt} is the melting temperature of the respective material. On the free surface and the rest of the fluid domain's boundary (that is on $\partial\Omega_f \setminus \overline{\Sigma_s}$), the previously given boundary conditions apply, e.g., Dirichlet, Newton's law, or Boltzmann radiation type boundary conditions.

We now address the characterization of the free surface and appropriate boundary conditions. Let us denote by

$$\mathcal{T} = -pI + \eta(\nabla\mathbf{u} + (\nabla\mathbf{u})^\top)$$

the total stress tensor of the fluid. We recall our equations on Ω_f

$$\begin{aligned} \rho \frac{\partial}{\partial t} \mathbf{u} - \eta \nabla \cdot (\nabla \mathbf{u} + (\nabla \mathbf{u})^\top) + \rho(\mathbf{u} \cdot \nabla) \mathbf{u} + \nabla p - \mathbf{J} \times \mathcal{B}(\mathbf{J}) \\ = \rho [1 - \beta(\Theta(\mathbf{u}, \mathbf{J}) - T_{\text{ref}})] \mathbf{g}, \\ \nabla \cdot \mathbf{u} = 0, \\ \frac{\partial}{\partial t} \mathcal{A}(\mathbf{J}) + \sigma^{-1} \mathbf{J} + \nabla \phi - \mathbf{u} \times \mathcal{B}(\mathbf{J}) = 0, \\ \nabla \cdot \mathbf{J} = 0, \end{aligned}$$

where for convenience we replaced the $\Delta \mathbf{u}$ term in the momentum equation

by the equivalent term $\nabla \cdot (\nabla \mathbf{u} + (\nabla \mathbf{u})^\top)$ so that the conditions imposed on the stress below become natural boundary conditions.

As in Section 2.1, we impose a Dirichlet boundary condition on the velocity

$$\mathbf{u}|_{\partial\Omega_f \setminus \bar{\Sigma}_f} = \mathbf{u}_b \quad (16)$$

at the crucible and crystal surfaces, where the given boundary velocity \mathbf{u}_b may be time-dependent and accounts for possible rotation of the crucible and the crystal ingot. We again impose (6) as boundary conditions for the current.

We describe the deviation of the free surface Σ_f from a flat surface (the fluid's top surface when at rest) as the graph of some time-dependent function H which is defined on $\Gamma_f \times (0, t_{\text{end}})$, where Γ_f is the projection of Σ_f onto the crucible's base Γ , see Figure 1. In order to determine H and to specify the fluid boundary conditions on the free surface, we need to provide four scalar equations, see, for example, [5, 20]. For free interfaces, conditions on the jump of the stress tensor across the interface are appropriate. The equilibration of forces across the free surface is modeled as being instantaneous, in accordance with previous work, see for instance [5, 8, 16]. Note that since the surrounding atmosphere is at rest, its total stress tensor is simply $-p_{\text{atm}}I$ where p_{atm} is the atmospheric pressure. The surface curvature is given by the expression

$$\nabla' \cdot \frac{\nabla' H}{\sqrt{1 + |\nabla' H|^2}},$$

where $\nabla' \cdot (\cdot)$ and $\nabla'(\cdot)$ are the surface divergence and gradient, respectively. The first equation is the Laplace-Young equation which states that the jump of the normal stresses across the interface is equal to the product of the surface tension coefficient γ and the curvature of the interface

$$\begin{aligned} -\gamma \nabla' \cdot \frac{\nabla' H}{\sqrt{1 + |\nabla' H|^2}} + p_{\text{atm}} &= -(\mathcal{T} \mathbf{n}) \cdot \mathbf{n} \\ &= p - \eta ((\nabla \mathbf{u} + (\nabla \mathbf{u})^\top) \mathbf{n}) \cdot \mathbf{n} \quad \text{on } \Gamma_f. \end{aligned} \quad (17)$$

Note that in the above equation, we abuse notation since some of the terms are to be evaluated on the free surface Σ_f rather than on its projection Γ_f .

The second and third conditions determine the jump of the tangential stresses across the free surface by equating it with the gradient of the surface tension γ . In our model, we account for variations in γ with temperature. These variations give rise to the so-called Marangoni effect, which can be sig-

nificant in crystal growth problems [16, 17]. We obtain

$$\mathcal{T}\mathbf{n} - ((\mathcal{T}\mathbf{n}) \cdot \mathbf{n})\mathbf{n} = \frac{d\gamma}{dT} \left(\nabla\Theta(\mathbf{u}, \mathbf{J}) - (\nabla\Theta(\mathbf{u}, \mathbf{J}) \cdot \mathbf{n})\mathbf{n} \right) \quad \text{on } \Sigma_f. \quad (18)$$

Note that (18) yields non-trivial conditions only in directions perpendicular to the surface normal \mathbf{n} and that if γ is constant the tangential stress vanishes.

As the fourth and final condition, we impose the kinematic constraint that the fluid velocity on the free surface is equal to that of the free surface, in the direction normal to the surface, i.e.,

$$\mathbf{u} \cdot \mathbf{n} = \frac{\partial H}{\partial t} (0, 0, 1)^\top \cdot \mathbf{n},$$

where $\mathbf{n} = \frac{(-\nabla'H, 1)^\top}{\sqrt{1+|\nabla'H|^2}}$ is the surface unit normal vector. This yields

$$\frac{\partial H}{\partial t} + (u_1, u_2) \cdot \nabla'H - u_3 = 0 \quad (19)$$

for all times t .

The above equations must be complemented by a boundary condition, an initial condition, and a constraint (which enforces mass conservation). In particular, equation (17) is a second order equation which must be complemented by a boundary condition

$$\frac{\nabla'H}{\sqrt{1+|\nabla'H|^2}} \cdot \mathbf{n}'|_{\partial\Gamma_f} = \cos \alpha(\Theta(\mathbf{u}, \mathbf{J})) \quad (20)$$

at all times, see [7]. Here $\partial\Gamma_f$ is the projection of $\partial\Sigma_f$ onto Γ and \mathbf{n}' is the planar outward pointing unit normal vector to Γ_f . The curves $\partial\Sigma_f$ are the so-called contact lines, i.e., the curves along which the fluid's free surface comes in contact with the container wall and the solid crystal, see Figure 1. Thus the condition (20) is a condition on the contact angle, which is in general temperature-dependent. It is also a material property which may be affected by surface treatments, see [7]. Equation (19) must be complemented by the initial condition

$$H(\mathbf{x}, 0) = 0 \quad \text{on } \Gamma_f. \quad (21)$$

The constraint alluded to above

$$\int_{\Gamma_f} H(\mathbf{x}, t) dx = 0 \quad (22)$$

for all times t , enforces the conservation of the fluid volume. Together these equations determine the location of the free surface.

Note that here we continue to employ the underlying assumption from the Boussinesq approximation, that the density is constant except in the buoyancy term. In addition, we have assumed that the consumption of melt due to crystallization, in the time window under consideration, is negligible compared to the volume of the liquid pool. If the consumption of melt cannot be neglected the constraint (22) must be adjusted to account for the loss of fluid which is related to the pull velocity.

3 Optimization

The free surface model described above can serve as the basis for numerical computations. Note that due to the velocity-current formulation, all unknown quantities are confined to the fluid domain Ω_f . On the one hand, numerical simulations can improve the understanding of the complex phenomena and interactions in the Czochralski growth process, compare, e.g., [16, 17].

On the other hand, there is a strong interest in optimizing crystal growth processes with respect to production rate and product quality. To this end, one has a number of parameters and time-dependent control functions at one's disposal. These include

- the heat sources, modeled either through q in (11), or an additional source term in the boundary condition (12),
- the crucible and crystal rotation speeds, represented by \mathbf{u}_b in (16),
- an electric potential difference applied to some electrodes attached to the fluid container, or a normal current injected into the fluid through these electrodes,
- the location, strength and configuration of applied magnetic fields \mathbf{B}_0 , see (8)–(9),
- the initial conditions, in particular \mathbf{T}_* for the temperature in (13),
- the geometry of the crucible Ω_f ,
- the pulling speed of the growing crystal.

For details and examples we refer to [11, 24, 25, 35, 36, 38]. Clearly, most of the variables above appear directly in our model described in Section 2. However, an applied magnetic field \mathbf{B}_0 can not be shaped at will. Therefore, a more detailed model of available coils etc. must be set up if these are subject to

optimization in a concrete situation. Likewise, an extension of our model is necessary in order to use the pulling speed as an optimization variable.

The optimal control of a crystal growth process has product quality and production rate as its ultimate objectives, and suitable optimization criteria need to be defined. So far, the attempts at optimizing CZ and related processes seem to be based on indirect quality indicators (which are to be maximized or minimized). Indirect indicators include, e.g., the deviation of the flow field from a desired one (known to produce favorable growth conditions), expressed by the objective functional

$$\min \int_0^{t_{\text{end}}} \int_{\Omega_f} |\mathbf{u} - \mathbf{u}_d|^2 dx dt,$$

where \mathbf{u}_d is a desired velocity field, e.g., that of rigid body rotation, compare [39]. To promote undisturbed growth, the reduction of “vorticity” may be desired, which leads to

$$\min \int_0^{t_{\text{end}}} \int_{\Omega_f} |\nabla \times \mathbf{u}|^2 dx dt.$$

Recently, also different vorticity-related functionals have been proposed for optimization in [18]. Since large temperature gradients may have an adverse effect on the growing crystal, one may also consider

$$\min \int_0^{t_{\text{end}}} \int_{\Omega_f} |\nabla T|^2 dx dt$$

as an objective. The optimization of all of these and similar objectives may be carried out using the model in Section 2, which focuses on the fluid/magnetic field interaction as stated in the introduction. For details concerning the analysis for a generic optimal control problem in the stationary case, including the derivation of adjoint equations, we refer to [9].

The use of direct quality indicators, such as dopant distribution, as the basis for optimization is major challenge which requires more advanced mathematical models.

References

- [1] A. Bermúdez and M. C. Muñiz. Numerical solution of a free boundary problem taking place in electromagnetic casting. *Mathematical Models and Methods in Applied Sciences*, 9(9):1393–1416, 1999.
- [2] A. Bermúdez, M. C. Muñiz, and P. Quintela. Existence and uniqueness for a free boundary problem in aluminum electrolysis. *J. Math. Anal. Appl.*, 191(3):497–527, 1995.

- [3] O. Besson, J. Borgeois, P.-A. Chevalier, J. Rappaz, and R. Touzani. Numerical modeling of electromagnetic casting processes. *Journal of Computational Physics*, 92:482–507, 1991.
- [4] M. Charina, A. J. Meir, and P. G. Schmidt. Mixed velocity, stress, current, and potential boundary conditions for stationary MHD flow. *Computers Math. Appl.*, 48:1181–1190, 2004.
- [5] C. Cuvelier. A capillary free boundary problem governed by the Navier-Stokes equations. *Comput. Methods Appl. Mech. Engrg.*, 48(1):45–80, 1985.
- [6] J. Descloux, M. Flueck, and M. V. Romerio. A modelling of the stability of aluminium electrolysis cells. In *Nonlinear partial differential equations and their applications. Collège de France Seminar, Vol. XIII (Paris, 1994/1996)*, volume 391 of *Pitman Res. Notes Math. Ser.*, pages 117–133. Longman, Harlow, 1998.
- [7] R. Finn. Capillary surface interfaces. *Notices of the AMS*, 46(7):770–781, 1999.
- [8] J.-F. Gerbeau, C. Le Bris, and T. Lelièvre. Simulations of MHD flows with moving interfaces. *Journal of Computational Physics*, 184(1):163–191, 2003.
- [9] R. Griesse and K. Kunisch. Optimal control for a stationary MHD system in velocity–current formulation. *SIAM Journal on Control and Optimization*, 45(5):1822–1845, 2006.
- [10] R. Griesse and A. J. Meir. Modeling of an MHD free surface problem arising in CZ crystal growth. In I. Troch and F. Breiteneker, editors, *5th IMACS Symposium on Mathematical Modelling—5th MATHMOD Vienna*, ARGESIM Reports, 2006. ISBN 3-901608-30-3.
- [11] M. Gunzburger, E. Ozugurlu, J. Turner, and H. Zhang. Controlling transport phenomena in the czochralski crystal growth process. *Journal of Crystal Growth*, 234:47–62, 2002.
- [12] S. Gupta. *The Classical Stefan Problem. Basic Concepts, Modelling and Analysis*, volume 45 of *Applied Mathematics and Mechanics*. North-Holland, Amsterdam, 2003.
- [13] H. Hirata and K. Hoshikawa. Silicon crystal growth in a cusp magnetic field. *Journal of Crystal Growth*, 96:745–755, 1989.
- [14] O. Klein, C. Lechner, P.-E. Druet, P. Philip, J. Sprekels, C. Frank-Rotsch, F. Kießling, W. Miller, U. Rehse, and P. Rudolph. Numerical simulation of Czochralski crystal growth under the influence of a traveling magnetic field generated by an internal heater-magnet module (HMM). *Journal of Crystal Growth*, 310(7–9):1523–1543, 2007.
- [15] O. Klein and P. Philip. Transient conductive-radiative heat transfer: Discrete existence and uniqueness for a finite volume scheme. *Mathematical Models and Methods in Applied Sciences*, 15(2):227–258, 2005.
- [16] V. Kumar, B. Basu, S. Enger, G. Brenner, and F. Durst. Role of Marangoni convection in Si-Czochralski melts—Part I: 3d predictions with crystal rotation. *Journal of Crystal Growth*, 255:27–39, 2003.
- [17] V. Kumar, B. Basu, S. Enger, G. Brenner, and F. Durst. Role of Marangoni convection in Si-Czochralski melts—Part II: 3d predictions without crystal. *Journal of Crystal Growth*, 253:142–154, 2003.
- [18] K. Kunisch and B. Vexler. Optimal vortex reduction for instationary flows based on translation invariant cost functions. *submitted*, 2005.
- [19] M. Laitinen and T. Tiihonen. Conductive-radiative heat transfer in grey materials. *Quarterly of Applied Mathematics*, 59(4):737–768, 2001.
- [20] L. D. Landau and E. M. Lifshitz. *Fluid Mechanics*, volume 6 of *Course of Theoretical Physics*. Pergamon Press, Oxford, second edition, 1987.
- [21] A. J. Meir and P. G. Schmidt. Variational methods for stationary MHD flow under natural interface conditions. *Nonlinear Anal.*, 26(4):659–689, 1996.
- [22] A. J. Meir and P. G. Schmidt. Analysis and numerical approximation of a stationary MHD flow problem with nonideal boundary. *SIAM J. Numer. Anal.*, 36(4):1304–1332, 1999.
- [23] A. J. Meir, P. G. Schmidt, S. I. Bhaktiyarov, and R. A. Overfelt. Numerical simulation of steady liquid-metal flow in the presence of a static magnetic field. *Trans. ASME J. Appl. Mech.*, 71(6):786–795, 2004.
- [24] M. Metzger. Optimal control of crystal growth processes. *Journal of Crystal Growth*, 23(1–2):210–216, 2001.
- [25] C. Meyer and P. Philip. Optimizing the temperature profile during sublimation growth of six single crystals: Control of heating power, frequency, and coil position. *Crystal Growth & Design*, 5(3):1145–1156, 2005.
- [26] P. Philip. *Transient Numerical Simulation of Sublimation Growth of SiC Bulk Single Crystals*. PhD thesis, Humboldt University of Berlin, 2003.
- [27] V. Prasad, H. Zhang, and A. P. Anselmo. Transport phenomena in Czochralski crystal growth processes. In *Advances in heat transfer*, volume 30, pages 313–435. Academic Press, 1997.
- [28] P. Prescott and F. Incropera. Magnetically damped convection during solidification of a binary

- metal alloy. *Journal of Heat Transfer*, 115:302–309, 1993.
- [29] J. Rappaz and R. Touzani. On a two-dimensional magnetohydrodynamic problem I. modeling and analysis. *M2AN Mathematical Modeling and Numerical Analysis*, 26(2):347–364, 1991.
- [30] J. Rappaz and R. Touzani. On a two-dimensional magnetohydrodynamic problem II. numerical analysis. *M2AN Mathematical Modeling and Numerical Analysis*, 30(2):215–235, 1996.
- [31] P. G. Schmidt. A Galerkin method for time-dependent MHD flow with nonideal boundaries. *Commun. Appl. Anal.*, 3:383–398, 1999.
- [32] R. W. Series. Effects of a shaped magnetic field in Czochralski silicon growth. *Journal of Crystal Growth*, 97:92–98, 1989.
- [33] R. W. Series and D. T. J. Hurle. The use of magnetic fields in semiconductor crystal growth. *Journal of Crystal Growth*, 113:305–328, 1991.
- [34] W. A. Tiller. *The Science of Crystallization*. Cambridge University Press, Cambridge, 1989.
- [35] J. Turner. Modelling control of crystal growth processes. *Computers & Mathematics with Applications*, 48(7–8):1231–1243, 2004.
- [36] A. Voigt and K.-H. Hoffmann. Control of Czochralski crystal growth. In *Optimal control of complex structures (Oberwolfach, 2000)*, volume 139 of *Internat. Ser. Numer. Math.*, pages 259–265. Birkhäuser, Basel, 2002.
- [37] J. S. Walker, D. Henry, and H. Ben Hadid. Magnetic stabilization of the buoyant convection in the liquid-encapsulated Czochralski process. *Journal of Crystal Growth*, 243:108–116, 2002.
- [38] C. Wang, H. Zhand, T. Wang, and L. Zheng. Solidification interface shape control in a continuous Czochralski silicon growth system. *Journal of Crystal Growth*, 287(2):252–257, 2006.
- [39] L. M. Witkowski and J. S. Walker. Numerical solutions for the liquid-metal flow in a rotating cylinder with a weak transverse magnetic field. *Fluid Dynamics Research*, 30:127–137, 2002.
- [40] L. M. Witkowski, J. S. Walker, and P. Marty. Nonaxisymmetric flow in a finite-length cylinder with a rotating magnetic field. *Physics of Fluids*, 11:1821–1826, 1999.